Energy & Environmental Science

Accepted Manuscript

ROYAL SOCIETY OF CHEMISTRY

www.rsc.org/ees

Journal Name

RSCPublishing

ARTICLE

Monodentate hydroxide as a super strong yet reversible active site for CO_2 capture from high-humidity flue gas

Cite this: DOI: 10.1039/x0xx00000x

Received 00th January 2012,
Accepted 00th January 2012

DOI: 10.1039/x0xx00000x

www.rsc.org/

Pei-Qin Liao, Huayao Chen, Dong-Dong Zhou, Si-Yang Liu, Chun-Ting He, Zebao Rui, Hongbing Ji, Jie-Peng Zhang* and Xiao-Ming Chen

We demonstrate here that porous coordination frameworks, functionalized with monodentate hydroxide on the pore surface, can achieve ultrahigh CO_2 adsorption affinity (124 kJ mol^{-1}), adsorption capacity (9.1 mmol cm^{-3} at 298 K and 1 bar), and CO_2/N_2 selectivity (262 at 298 K) by reversible formation/decomposition of bicarbonate in the adsorption/desorption processes. More importantly, these materials can capture up to 4.1 mmol cm^{-3} or 13.4 wt% of CO_2 from simulated flue gases (CO_2 pressure 0.10-0.15 bar at 313 K) even at high relative humidity (82%), and quickly release them under mild regeneration condition (N_2 purge at 358 K), representing the best CO_2 capture performances reported to date.

Introduction

Capturing CO_2 from flue gas by solid adsorbents is a rapidly growing research topic.[1-4] The performance of adsorbent is usually evaluated by the CO_2 adsorption capacity and CO_2/N_2 selectivity,[5] which are determined mainly by their CO_2 binding affinity.[6] It should be noted that, although the adsorption capacities are generally calculated against the weights of the adsorbents (i.e., gravimetric adsorption capacity), the volumetric adsorption capacity is more practical for the stationary CO_2 capture and separation applications,[7, 8] and also reflects the CO_2 binding affinity straightforwardly. Easy regeneration condition (low energy cost) and high tolerance against humidity (both framework stability and adsorption performance) are also crucial characteristics for practical applications yet rarely observed.[9, 10]

The designable and modifiable pore surfaces of porous coordination polymers (PCPs) or metal-organic frameworks (MOFs) are very attractive for CO_2 capture.[11-35] To improve the CO_2 adsorption affinities and capacities, various types of pore-surface active sites have been explored, in which open metal site (OMS) and alkylamine group are the most effective ones so far (Table S1).[7, 11, 12, 36-38] For examples, because of the low crystal density and strong Lewis acidity of OMSs, [Mg_2(dobdc)] and [Co_2(dobdc)] (H_4dobdc = 2,5-dihydroxyl-1,4-benzenedicarboxylic acid) hold the records of gravimetric (8.0 mmol g^{-1}) and volumetric (8.2 mmol cm^{-3}) CO_2 adsorption capacities (at 298 K and 1 bar), respectively.[13] On the other hand, the highest CO_2/N_2 selectivities[5] (>200) have been reported for alkylamine functionalized adsorbents, since they interact chemically with CO_2 but weakly with N_2.[11, 38-40] It should be noted that, high adsorption enthalpies are generally associated with high regeneration temperatures and energy costs, although the consumed energy is mainly used to elevate the temperature of the adsorbent (proportional to the heat capacity).[6, 7]

Hydroxide anion is a well-known species for its extremely high affinity to CO_2 (heat of formation of HCO_3^- from OH^- and CO_2 in the gas phase is ca. 205 kJ mol^{-1}),[41] but the irreversible chemical reaction is unsuitable for practical CO_2 capture/separation applications. A monodentate hydroxide may be a good candidate combining strong CO_2 affinity and reaction reversibility, considering that it is the key active site of carbonic anhydrase which can greatly accelerate the conversion between CO_2 and HCO_3^- in aqueous environment without altering the thermodynamic equilibrium. However, hydroxide ligands are generally bidentate or tridentate in coordination complexes, which possess poor Lewis basicity for CO_2 binding.[8, 42] Only very few PCPs consisting of monodentate hydroxide have been reported and/or deposited in the crystal structure database,[43-47] but their CO_2 capture performances are either poor (indicating that they are not really monodentate hydroxide) or not studied. Actually, it is very difficult to confirm the presence of monodentate hydroxide anion by means of X-ray crystallography. Here, we report the first unambiguous evidences of the extraordinary CO_2 capture performances of this new type of active site, based on an in-depth comparison study of a unique set of isostructural PCPs (Figure 1), namely [$Mn^{II}_2Cl_2$(bbta)] (H_2bbta = 1*H*,5*H*-benzo(1,2-d:4,5-d')bistriazole, MAF-X25, **1**)[48] and [$Co^{II}_2Cl_2$(bbta)] (MAF-X27, **2**), [$Mn^{II}Mn^{III}$(OH)Cl_2(bbta)] (MAF-X25ox, **1'**),[48] and [$Co^{II}Co^{III}$(OH)Cl_2(bbta)] (MAF-X27ox, **2'**).

Results and discussion

The crystal structures and sample quality of microcrystalline **1**, **2**, **1'**, and **2'** were characterized by Rietveld refinements of their powder X-ray diffraction (PXRD) patterns (Fig. S1 and S2 and Table S2). Because the ionic radius follows M(III) < M(II) and Co < Mn, their unit-cell volumes follow **2'** < **2** < **1'** < **1**. Comparison of the crystal structures showed that the coordination environments changed from square-pyramidal MN_3Cl_2 in **1**/**2** to octahedral MN_3Cl_2O in **1'**/**2'**, concomitant with about 0.03 Å reduction of the coordination bond lengths, which confirmed the oxidation of metal ions. Infrared (IR) spectroscopy showed the characteristic stretching vibration for the OH^- ions in **1'** and **2'** (Fig. S3).[43, 49] The refinements revealed ca. half occupancies for the OH^- groups in **1'**/**2'**, indicating that they were composed of about statistically distributed M(II) and M(III)-OH sites with 1:1 molar ratio (Fig. 1). Their chemical compositions and framework structures were further confirmed by X-ray photoelectron spectroscopy (Fig. S4), electron paramagnetic resonance spectroscopy and (Fig. S5) room temperature magnetic susceptibility, elemental analyses (Table S3), and/or N_2 sorption measurements.

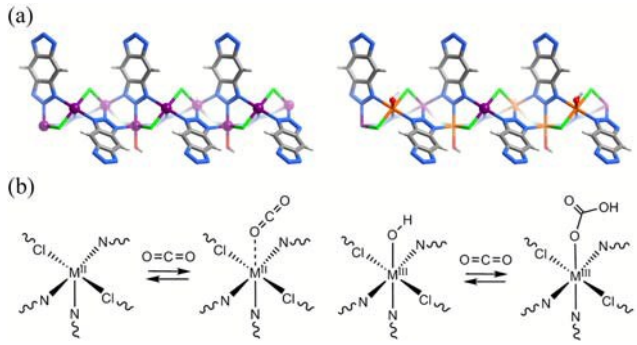

Fig. 1 Comparison of the (a) local framework structures (C, gray; H, light gray; N, blue; O, red; M(II), purple; M(III) orange) and (b) CO_2 adsorption mechanisms of **1**/**2** and **1'**/**2'**.

N_2 sorption isotherms measured at 77 K gave apparent Langmuir surface areas of 1566, 1407, 1286, and 1167 $m^2\ g^{-1}$, and pore volumes of 0.56, 0.52, 0.46, and 0.41 $cm^3\ g^{-1}$, respectively, for **1**, **2**, **1'**, and **2'** (Fig. S6). Considering that their crystallographic pore volumes are 0.56, 0.50, 0.44, and 0.40 $cm^3\ g^{-1}$, respectively (Table S2), the N_2 sorption data further confirmed the good sample crystallinity and purity.

The CO_2 sorption properties of **1**, **2**, **1'**, and **2'** were studied at conditions close to the flue gas environments. At 298 K and 1 bar, **1** and **2** have CO_2 uptakes of 5.36 and 4.24 mmol g^{-1}, respectively (Fig. 2a), which are relatively high values in the literature,[6] but much lower than those of [M_2(dobdc)] (Table S1). Compared with [M_2(dobdc)] based on oxygen donors, the weaker CO_2 affinities of **1** and **2** can be ascribed to the lower electronegativities of chloride and nitrogen, which reduce the Lewis acidity of metal ions and the polarity of the pore surface. The CO_2 uptake of **1** is obviously higher than that of **2** over all pressures, which can be ascribed to not only the lighter weight and larger pore volume, but also the stronger acidity of Mn(II) in **1** (Fig. S7a).

1' and **2'** show remarkably enhanced CO_2 binding affinities, as reflected by the large slopes at low pressures, large uptakes at all pressures, and hysteresis loops of the isotherms (Fig. 2a). For example, at 298 K and 1 bar, **1'** and **2'** adsorbed 7.1 and 6.7 mmol g^{-1}, which are about 30% and 50% higher than those of **1** and **2**, respectively. The gravimetric CO_2 uptakes of **1'** and **2'** are comparable with [Co_2(dobdc)] (6.9 mmol g^{-1}) and only lower than that of [Mg_2(dobdc)] mainly because of the much lighter weight of Mg. In the volumetric point of view, the adsorption capacity of **1'** and **2'** are 8.7 and 9.1 mmol cm^{-3} at 298 K and 1 bar, which are the highest values reported to date. At 298 K and 0.15 bar, the volumetric capacity of **1'** and **2'** reach 5.0 and 5.5 mmol cm^{-3}, which are 410% and 540% higher than those of **1** and **2**, respectively.[6, 13] Compared with **1** and **2**, the much higher CO_2 uptakes of **1'** and **2'** should be explained by the strong interaction between M(III)-OH and CO_2. It should be noted that the adsorption isotherms of **1'** and **2'** are quite similar. At the low pressure region, the CO_2 adsorption of **2'** is even slightly stronger than that of **1'** (Fig. S7b), which is in contrast to the difference between **1** and **2**. This phenomenon can be ascribed to the fact that both **1'** and **2'** have the same OH^- active sites, so that their CO_2 adsorption behaviors are mainly controlled by the pore size and volumes.

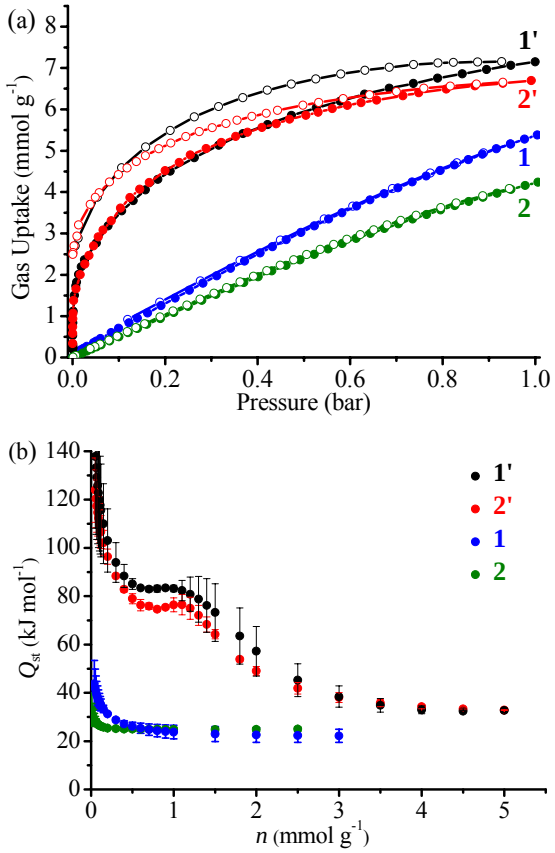

Fig. 2 (a) CO_2 adsorption (solid) and desorption (open) isotherms measured at 298 K and (b) coverage-dependent CO_2 adsorption enthalpy (obtained by the dual-site Langmuir-Freundlich fitting) for **1**, **2**, **1'**, and **2'**.

The coverage-dependent CO_2 adsorption enthalpy (Q_{st}) of **1**, **2**, **1'**, and **2'** were obtained by Virial and dual-site Langmuir-Freundlich (DSLF) analyses of the adsorption isotherms measured at three

different temperatures (Figs 2b and S8-S14). For **1** and **2**, , the Virial/DSLF method gave Q_{st} = 38/43 and 28/33 kJ mol^{-1} at zero coverage, respectively, which are lower than the values of other PCPs functionalized with O-coordinated OMSs, confirming their relatively low Lewis acidity of N/Cl-coordinated OMSs. For **1'** and **2'**, the Virial/DSLF method gave Q_{st} = 99/120 and 110/124 kJ mol^{-1} at zero coverage, respectively (Table S1). The ultrahigh CO_2 affinities of **1'** and **2'** can be assigned to chemisorption interaction.[50] *In situ* IR spectra of **2'** with varied atmosphere were measured to study the CO_2 capture mechanism (Fig. S15). In CO_2 atmosphere, the stretching vibration of HO^- at 3605 cm^{-1} disappears, and new adsorption bands characteristic for the stretching vibration of CO−H of HCO_3^- at 3682 cm^{-1}, the symmetrical stretching vibration of O=C−O of HCO_3^- at 1224 cm^{-1}, as well as bending vibration of CO−H of HCO_3^- at 1050 cm^{-1} appear.[51, 52]

To study the CO_2/N_2 selectivity, N_2 sorption isotherms for **1**, **2**, **1'**, and **2'** were also measured at 298 K, which showed uptakes of 0.29, 0.22, 0.10, and 0.06 mmol g^{-1} at 1 bar, respectively (Fig. S16). In contrast to the cases of CO_2 adsorption, **1'**/**2'** adsorb less N_2 than **1**/**2**, which can be explained by the relatively high N_2 affinity of OMS,[6] as well as the low N_2 affinity of hydroxide. The CO_2/N_2 selectivities of **1**, **2**, **1'**, and **2'** at 298 K were calculated[5] to be 26, 24, 250, and 262, respectively (Table S1).[7, 11, 38-40]

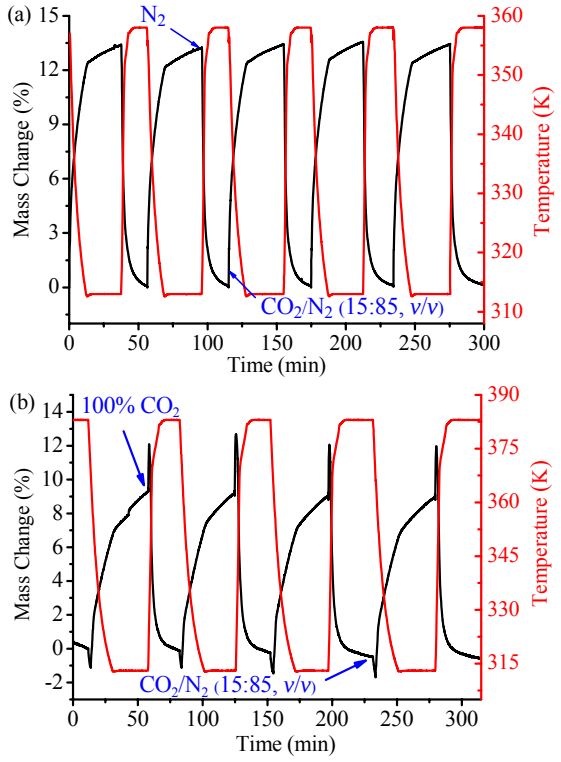

Fig. 3 Repeated adsorption–desorption kinetics for **2'** between a 15:85 CO_2/N_2 (*v*/*v*) flow at 313 K and (a) a pure N_2 flow at 358 K, or (b) a pure CO_2 flow at 383 K.

The CO_2 adsorption and desorption behaviors of **1'** and **2'** under mixed-gas and kinetic conditions were analyzed by thermogravimetry (Figs 3a and S17), in which the adsorbents were blown repeatedly using a 15:85 CO_2/N_2 (*v*/*v*) mixture at 313 K (a typical flue gas environment) and a pure N_2 flow (a typical regeneration method for temperature-vacuum swing adsorption (TVSA) like process) at 358 K (optimized). The maximum and repeatable weight changes of **1'** and **2'** were about 13.1 and 13.4 wt%, corresponding to volumetric uptakes of 3.7 and 4.1 mmol cm^{-3}, respectively. Although such mixed-gas adsorption measurement is much more relevant with practical CO_2 capture applications under flue gas conditions, it has been rarely reported in the literature, in which the highest gravimetric and volumetric uptakes were 14.6 wt% and 3.2 mmol cm^{-3}, respectively, achieved by $[Mg_2(dobpdc)(en)_{1.6}]$ (en-Mg_2(dobpdc), en = ethylenediamine, H_4dobpdc = 4,4'-dihydroxy-(1,1'-biphenyl)-3,3'-dicarboxylic acid) at a much higher desorption temperature of 423 K (Table S4).

A pure temperature swing adsorption (TSA) process for **2'** was further carried out, and the working capacity was obtained as 2.0 mmol g^{-1} between 15:85 CO_2/N_2 (*v*/*v*) mixture at 313 K and a pure CO_2 flow at 383 K (optimized). To evaluate the regeneration energy, heat capacity was quantified for **2'** via differential scanning calorimetry. About −98 J g^{-1} was evolved as the material was cooled from 383 to 313 K (Fig. S18). With these data (see calculation method in the Supporting Information), approximately 2.7 MJ of energy would be required to regenerate 1 kg of CO_2 adsorbed onto **2'** (Fig. 3b).[36, 38] It should be noted that, the CO_2 adsorption and desorption by **1'** and/or **2'** under TVSA and TSA processes are very fast, which are exceptional considering the very high CO_2 affinity of the adsorbents.

To simulate practical CO_2 capture applications, we also measured and compared the breakthrough curves of **2** and **2'** by using binary 10:90 CO_2/N_2 (*v*/*v*) mixture at 313 K and 1 bar. By virtue of the extraordinary CO2 adsorption property of **2'**, good experimental results can be obtained at the real flue gas temperature, while previous reports were carried out at 298 K.[10, 12, 23, 53, 54] To present and compare the performances of the materials unambiguously, we used the specific injection amount (mmol g^{-1}) of the mixed gas as the abscissa (Figs 4, S19 and S20), meaning that the breakthrough time (s) was not only divided by the adsorbent weight (g) but also multiplied by the flow rate of the injected mixed gas (mmol s^{-1}).

As shown in Fig. 4, N_2 can be detected at the outlet quickly (<0.5 mmol g^{-1}), and the outlet N_2 concentrations quickly reached the inlet one at ca. 2-3 mmol g^{-1}, indicating that the columns interact weakly with N_2 so that the remnant He (used to activate and protect the column) gas was effectively washed out. The breakthrough curves confirmed that the CO_2/N_2 selectivity of **2'** is much higher than for **2**. The breakthrough points of CO_2 for **2** and **2'** are ca. 2 and 22 mmol g^{-1}, respectively. Integration of the N_2 breakthrough curve to the CO_2 breakthrough point gives the amount of N_2 purified from the 10:90 CO_2/N_2 mixture by a single breakthrough operation, which is 2.7 mmol g^{-1} for **2** or 19 mmol g^{-1} for **2'**. After the breakthrough points, the outlet CO_2 concentrations rose gradually to those of the inlets at 8 and 28 mmol g^{-1} for **2** and **2'**, respectively. Based on the breakthrough curve, the amount of CO_2 adsorbed by the adsorbent in the column can be calculated (see calculation method in ESI) as 0.27 and 2.5 mmol g^{-1} for **2** and **2'**, respectively, which are 70% and 96% of the values obtained from the single-component adsorption isotherms (0.39 and 2.60 mmol g^{-1} at T = 313 K and P_{CO2} = 0.1 bar). These data indicate that under such a kinetic and mixed-gas condition **2'** can still work as good as it does under the thermodynamic and single-component condition, which should be

attributed to the high CO_2/N_2 selectivity and fast adsorption/desorption kinetics of **2'**. For comparison, the adsorption capacity of [Mg_2(dobdc)] is 4.07 mmol g^{-1} estimated by breakthrough experiment using 15:85 CO_2/N_2 (*v*/*v*) mixture at 298 K and 1 bar, but 5.43 mmol g^{-1} by single-component CO_2 adsorption isotherm at 0.15 bar and 298 K.[55]

Capturing CO_2 in the presence of water is an outstanding challenge. Although many materials can trap CO_2 in voluminous amounts under dry conditions, the efficiency of capture is significantly reduced in the presence of water, because water molecule competes for the binding site or destroys the framework.[11, 12] For instance, after being exposed to water vapor, the CO_2 adsorption capacity of [Mg_2(dobdc)] is reduced by about 50% even at dry condition.[11] Remarkably, the breakthrough curves of **2'** under dry and high-humidity conditions are almost the same,[10, 12, 23, 53] whereas **2** almost lost the ability to capture CO_2 from the wet gas mixture.[54] This difference can be easily understood by the very different affinities of OMS and hydroxide toward H_2O and CO_2. Such exceptionally high CO_2 affinity, CO_2 adsorption capacity, and CO_2/N_2 selectivity, under high-temperature and high-humidity flue gas conditions, highlighted the suitability of **2'** as a promising CO_2 capture adsorbent.

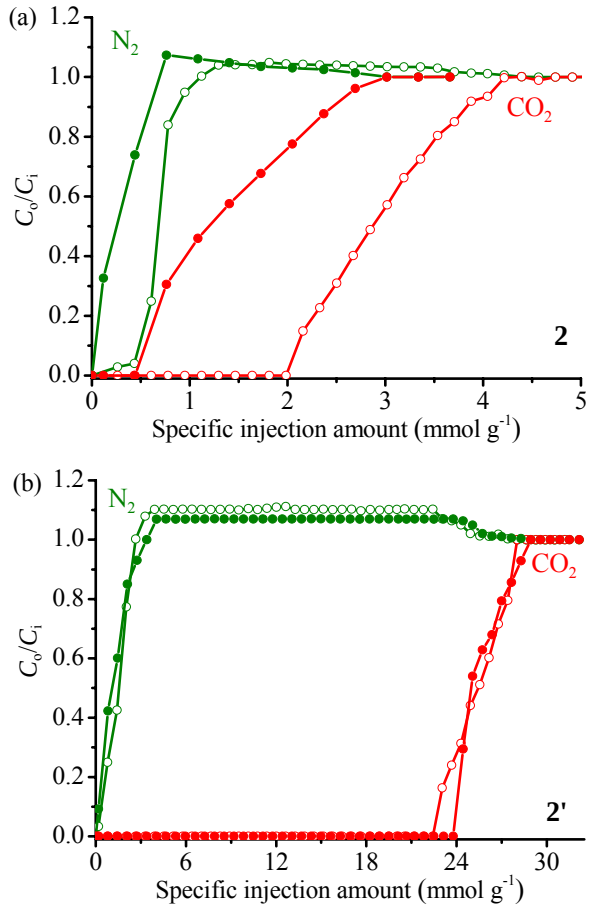

Fig. 4 Breakthrough curves for 10:90 CO_2/N_2 (*v*/*v*) mixture with 0% (open) and 82(3)% relative humidity (solid) at 313 K and 1 bar passing through a column packed by microcrystalline (a) **2** or (b) **2'**. Lines are drawn to guide eyes. C_i and C_o are the concentrations of each gas at the inlet and outlet, respectively.

Conclusions

In summary, we showed that PCPs functionalized by monodentate hydroxide on their pore surfaces of can serve as a very strong yet reversible active site for CO_2 capture. The prototypical PCPs showed not only ultrahigh CO_2 affinity/uptake and CO_2/N_2 selectivity, but also good recycling stability, very fast sorption kinetics and ultrahigh working capacity for capturing CO_2 under flue gas conditions, even in the presence of water. These results should be instructive for designing and discovering the next-generation adsorbents for efficient CO_2 separation and capture.

ACKNOWLEDGMENT

This work was supported by the "973 Project" (2012CB821706 and 2014CB845602), NSFC (21225105, 21371181, and 21473260).

Notes and references

MOE Key Laboratory of Bioinorganic and Synthetic Chemistry, School of Chemistry and Chemical Engineering, Sun Yat-Sen University, Guangzhou 510275, China.

† Electronic Supplementary Information (ESI) available: Experimental details, methods and additional discussions, thermogravimetry curves, PXRD patterns, Spectroscopy characterization, additional isotherms, as well as X-ray crystallographic data with CIF files. See DOI: 10.1039/b000000x/

1. J. Liu, P. K. Thallapally, B. P. McGrail, D. R. Brown and J. Liu, *Chem. Soc. Rev.*, 2012, **41**, 2308-2322.
2. D. M. D'Alessandro, B. Smit and J. R. Long, *Angew. Chem. Int. Ed.*, 2010, **49**, 6058-6082.
3. Z. Zhang, Z.-Z. Yao, S. Xiang and B. Chen, *Energy Environ. Sci.*, 2014, **7**, 2868-2899.
4. Z. Zhang, Y. Zhao, Q. Gong, Z. Li and J. Li, *Chem. Commun.*, 2013, **49**, 653-661.
5. The CO_2/N_2 selectivity is calculated by uptake ratios at the partial pressures of flue gas (CO_2 0.15 bar; $N1_2$ 10.75 bar) at 313 K.
6. K. teppeiSumida, D. L. Rogow, J. A. Mason, T. M. McDonald, E. D. Bloch, Z. R. Herm, T.-H. Bae and J. R. Long, *Chem. Rev.*, 2012, **112**, 724-781.
7. T. M. McDonald, D. M. D'Alessandro, R. Krishna and J. R. Long, *Chem. Sci.*, 2011, **2**, 2022-2028.
8. D.-D. Zhou, C.-T. He, P.-Q. Liao, W. Xue, W.-X. Zhang, H.-L. Zhou, J.-P. Zhang and X.-M. Chen, *Chem. Commun.*, 2013, **49**, 11728-11730.
9. P. K. Thallapally, R. K. Motkuri, C. A. Fernandez, B. P. McGrail and G. S. Behrooz, *Inorg. Chem.*, 2010, **49**, 4909-4915.
10. P. Nugent, Y. Belmabkhout, S. D. Burd, A. J. Cairns, R. Luebke, K. Forrest, T. Pham, S. Ma, B. Space, L. Wojtas, M. Eddaoudi and M. J. Zaworotko, *Nature*, 2013, **495**, 80-84.
11. W. R. Lee, S. Y. Hwang, D. W. Ryu, K. S. Lim, S. S. Han, D. Moon, J. Choi and C. S. Hong, *Energy Environ. Sci.*, 2014, **7**, 744-751.
12. A. M. Fracaroli, H. Furukawa, M. Suzuki, M. Dodd, S. Okajima, F. Gandara, J. A. Reimer and O. M. Yaghi, *J. Am. Chem. Soc.*, 2014, **136**, 8863-8866.

13. S. R. Caskey, A. G. Wong-Foy and A. J. Matzger, *J. Am. Chem. Soc.*, 2008, **130**, 10870-10871.
14. B. Li, Z. Zhang, Y. Li, K. Yao, Y. Zhu, Z. Deng, F. Yang, X. Zhou, G. Li, H. Wu, N. Nijem, Y. J. Chabal, Z. Lai, Y. Han, Z. Shi, S. Feng and J. Li, *Angew. Chem. Int. Ed.*, 2012, **51**, 1412-1415.
15. J.-R. Li, J. Yu, W. Lu, L.-B. Sun, J. Sculley, P. B. Balbuena and H.-C. Zhou, *Nat. Commun.*, 2013, **4**, 1538.
16. S. M. Cohen, *Chem. Rev.*, 2012, **112**, 970-1000.
17. Y. He, W. Zhou, R. Krishna and B. Chen, *Chem. Commun.*, 2012, **48**, 11813-11831.
18. T. Fukushima, S. Horike, Y. Inubushi, K. Nakagawa, Y. Kubota, M. Takata and S. Kitagawa, *Angew. Chem. Int. Ed.*, 2010, **49**, 4820-4824.
19. B. Zheng, J. Bai, J. Duan, L. Wojtas and M. J. Zaworotko, *J. Am. Chem. Soc.*, 2010, **133**, 748-751.
20. R. Vaidhyanathan, S. S. Iremonger, G. K. Shimizu, P. G. Boyd, S. Alavi and T. K. Woo, *Science*, 2010, **330**, 650-653.
21. M. Wriedt, J. P. Sculley, A. A. Yakovenko, Y. G. Ma, G. J. Halder, P. B. Balbuena and H. C. Zhou, *Angew. Chem. Int. Ed.*, 2012, **51**, 9804-9808.
22. P.-Q. Liao, D.-D. Zhou, A.-X. Zhu, L. Jiang, R.-B. Lin, J.-P. Zhang and X.-M. Chen, *J. Am. Chem. Soc.*, 2012, **134**, 17380-17383.
23. O. Shekhah, Y. Belmabkhout, Z. Chen, V. Guillerm, A. Cairns, K. Adil and M. Eddaoudi, *Nat. Commun.*, 2014, **5**, 4228.
24. J. A. Johnson, S. Chen, T. C. Reeson, Y. S. Chen, X. C. Zeng and J. Zhang, *Chem. Eur. J.*, 2014, **20**, 7632-7637.
25. J. An, S. J. Geib and N. L. Rosi, *J. Am. Chem. Soc.*, 2009, **132**, 38-39.
26. T. Panda, P. Pachfule, Y. Chen, J. Jiang and R. Banerjee, *Chem. Commun.*, 2011, **47**, 2011-2013.
27. T. Devic, F. Salles, S. Bourrelly, B. Moulin, G. Maurin, P. Horcajada, C. Serre, A. Vimont, J.-C. Lavalley, H. Leclerc, G. Clet, M. Daturi, P. L. Llewellyn, Y. Filinchuk and G. Férey, *J. Mater. Chem.*, 2012, **22**, 10266-10273.
28. C. R. Wade and M. Dincă, *Dalton. Trans.*, 2012, **41**, 7931-7938.
29. C. Montoro, E. Garcia, S. Calero, M. A. Perez-Fernandez, A. L. Lopez, E. Barea and J. A. R. Navarro, *J. Mater. Chem.*, 2012, **22**, 10155-10158.
30. H. J. Park and M. P. Suh, *Chem. Sci.*, 2013, **4**, 685-690.
31. L.-H. Xie and M. P. Suh, *Chem. Eur. J.*, 2013, **19**, 11590-11597.
32. S. Xiang, Y. He, Z. Zhang, H. Wu, W. Zhou, R. Krishna and B. Chen, *Nat. Commun.*, 2012, **3**, 954.
33. P. Wang, Y. Lu Yi, Q. Liu and W.-Y. Sun, *Scientia Sinica Chimica*, 2013, **43**, 1288-1296.
34. S. S. Nagarkar, A. K. Chaudhari and S. K. Ghosh, *Inorg. Chem.*, 2011, **51**, 572-576.
35. A. Khutia and C. Janiak, *Dalton. Trans.*, 2014, **43**, 1338-1347.
36. J. A. Mason, K. Sumida, Z. R. Herm, R. Krishna and J. R. Long, *Energy Environ. Sci*, 2011, **4**, 3030-3040.
37. A. Demessence, D. M. D'Alessandro, M. L. Foo and J. R. Long, *J. Am. Chem. Soc.*, 2009, **131**, 8784-8786.
38. T. M. McDonald, W. R. Lee, J. A. Mason, B. M. Wiers, C. S. Hong and J. R. Long, *J. Am. Chem. Soc.*, 2012, **134**, 7056-7065.
39. Y. Lin, Q. Yan, C. Kong and L. Chen, *Sci. Rep.*, 2013, **3**, 1859.
40. S. Sung and M. P. Suh, *J. Mater. Chem. A*, 2014, **2**, 13245-13249.
41. J. Y. Liang and W. N. Lipscomb, *J. Am. Chem. Soc.*, 1986, **108**, 5051-5058.
42. S. Yang, J. Sun, A. J. Ramirez-Cuesta, S. K. Callear, I. F. DavidWilliam, D. P. Anderson, R. Newby, A. J. Blake, J. E. Parker, C. C. Tang and M. Schröder, *Nat. Chem.*, 2012, **4**, 887-894.
43. D. J. Xiao, E. D. Bloch, J. A. Mason, W. L. Queen, M. R. Hudson, N. Planas, J. Borycz, A. L. Dzubak, P. Verma, K. Lee, F. Bonino, V. Crocellà, J. Yano, S. Bordiga, D. G. Truhlar, L. Gagliardi, C. M. Brown and J. R. Long, *Nat. Chem.*, 2014, **6**, 590-595.
44. W. Ouellette, M. H. Yu, C. J. O'Connor, D. Hagrman and J. Zubieta, *Angew. Chem. Int. Ed.*, 2006, **45**, 3497-3500.
45. A. Schoedel, A. J. Cairns, Y. Belmabkhout, L. Wojtas, M. Mohamed, Z. Zhang, D. M. Proserpio, M. Eddaoudi and M. J. Zaworotko, *Angew. Chem. Int. Ed.*, 2013, **52**, 2902-2905.
46. J. Zhang, J. T. Bu, S. Chen, T. Wu, S. Zheng, Y. Chen, R. A. Nieto, P. Feng and X. Bu, *Angew. Chem. Int. Ed.*, 2010, **49**, 8876-8879.
47. P. K. Allan, B. Xiao, S. J. Teat, J. W. Knight and R. E. Morris, *J. Am. Chem. Soc.*, 2010, **132**, 3605-3611.
48. P.-Q. Liao, X.-Y. Li, J. Bai, C.-T. He, D.-D. Zhou, W.-X. Zhang, J.-P. Zhang and X.-M. Chen, *Chem. Eur. J.*, 2014, **20**, 11303-11307.
49. S. W. Kim, B. J. Kwon, J. H. Park, M. G. Hur, S. D. Yang and H. Jung, *Bull. Korean Chem. Soc.*, 2010, **31**, 910-914.
50. D. N. Silverman and S. Lindskog, *Acc. Chem. Res.*, 1988, **21**, 30-36.
51. E. Garand, T. Wende, D. J. Goebbert, R. Bergmann, G. Meijer, D. M. Neumark and K. R. Asmis, *J. Am. Chem. Soc.*, 2009, **132**, 849-856.
52. D. A. Palmer and R. Van Eldik, *Chem. Rev.*, 1983, **83**, 651-731.
53. N. T. T. Nguyen, H. Furukawa, F. Gándara, H. T. Nguyen, K. E. Cordova and O. M. Yaghi, *Angew. Chem. Int. Ed.*, 2014, **53**, 10645-10648.
54. J. Liu, J. Tian, P. K. Thallapally and B. P. McGrail, *J. Phys. Chem. C*, 2012, **116**, 9575-9581.
55. D. A. Yang, H. Y. Cho, J. Kim, S. T. Yang and W. S. Ahn, *Energy Environ. Sci*, 2012, **5**, 6465-6473.